Gregory Richards Thesis Proposal: Investigating Pulsar Radiation at the Highest Energies

ABSTRACT

This thesis proposal details a plan comprising past, present, and future research with the VERITAS imaging atmospheric Cherenkov technique (IACT) telescope that aims primarily to investigate the nature of the highest energy electromagnetic radiation seen from pulsars. The recent detection of very-high-energy (VHE, E > 100 GeV) gamma-rays from the Crab pulsar has posed a novel and exciting challenge for experimentalists and theoreticians alike. In the time since its detection above 100 GeV with VERITAS, no other pulsar has been seen in the same energy band despite ongoing efforts by multiple IACT collaborations. To better understand the VHE emission mechanisms of pulsars, I plan to continue analysis of the ongoing VERITAS pulsar survey data in addition to conducting an extensive search for pulsed VHE emission from 13 pulsars in archival VERITAS data. Almost all of the pulsars mentioned within this proposal have never before been probed for VHE emission. The detection of just one new VHE gamma-ray-emitting pulsar would prove extremely valuable in shaping our understanding of magnetospheric particle acceleration mechanisms.

1. INTRODUCTION

1.1. Motivation for probing pulsars in the VHE gamma-ray band

Very-high-energy gamma-ray astronomy is a recently established and ever-growing field that aims to better understand relativistic particle acceleration mechanisms in the universe through gamma-ray detection. Following the detection of the Crab Nebula, the first confirmed VHE gamma-ray source (Weekes et al. 1989), the VHE source catalog has seen a rapid increase in number of over two orders of magnitude[1] with over 100 new members joining in just the last decade. The types of physics questions that can be addressed are far-reaching as relativistic acceleration appears now to be quite ubiquitous in the universe, but in this proposal I focus primarily on investigating magnetospheric acceleration of particles in pulsars through their gamma-ray radiation.

It was not until very recently that pulsars joined the VHE source class list with the paradigm-shifting detection of the Crab pulsar above 100 GeV with the Very Energetic Radiation Imaging Telescope Array System (VERITAS) (VERITAS Collaboration et al. 2011). As of this writing, this unprecedented detection remains the only detection of a pulsar in the very-high-energy band, and not surprisingly, the detection came as a huge surprise to the astronomical community. The spectral energy distributions (SEDs) that

[1] http://tevcat.uchicago.edu/

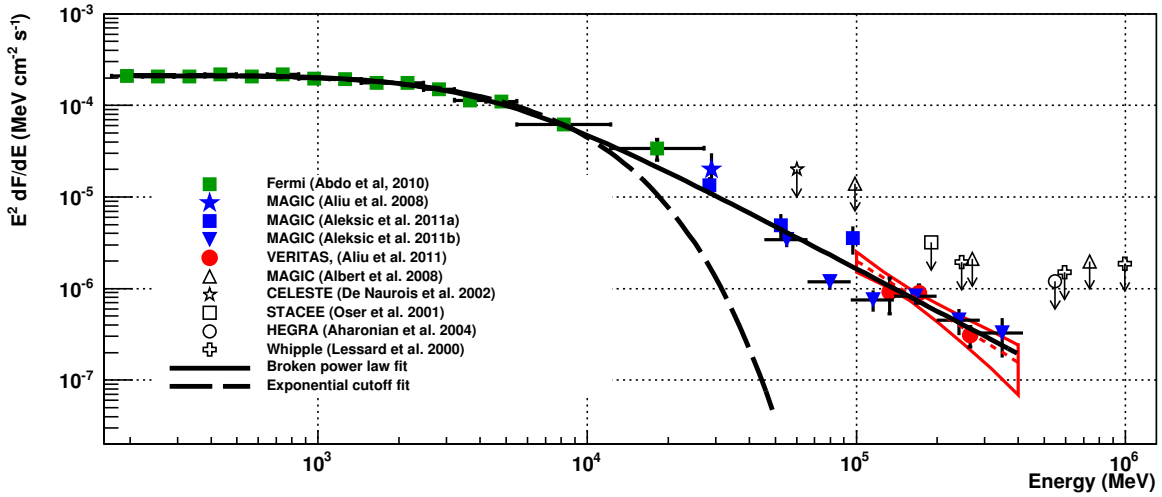

Fig. 1.— Crab pulsar spectral energy distribution for the energy range from 100 MeV to 400 GeV. Spectral measurements from *Fermi*-LAT, MAGIC, and VERITAS are shown along with upper limits from a other VHE gamma-ray instruments. The exponential cutoff fit to the *Fermi*-LAT data is clearly a poor description for the tail of the SED in light of the recent measurements by VERITAS and MAGIC. The exact nature and origin of the VHE gamma-ray emission remains an unsolved problem in the field.

have been seen for pulsars in gamma rays are all well-characterized by a broad curvature radiation component that originates due to the electrons and positrons that fill the magnetosphere and follow curved trajectories as they are confined to the magnetic field lines. A curvature radiation component has a natural end at GeV energies where the emission becomes radiation-reaction limited (Cheng et al. 1986). The spectral "tails" in the GeV band of pulsars detected by the *Fermi*-LAT (the large area telescope aboard the *Fermi* satellite) have all been well-described by an exponential cutoff as expected for curvature radiation (Abdo et al. 2013), though statistics are sparse above ~ 10 GeV due to the LAT's poor sensitivity at high energies. Based on the detection of the Crab pulsar above 100 GeV, it appears to be the case that curvature radiation is not adequate for a full explanation of the radiation from at least the Crab pulsar; the combined *Fermi*-LAT and VERITAS SED favors a power-law fit above ~ 10 GeV as can be seen in Figure 1.

It has become clear that in order to better understand the physics of gamma-ray radiation from pulsars, more research must be done in the VHE band. A detection of another pulsar at energies above 100 GeV would provide valuable new insight into the emission mechanisms, the geometry of the pulsar magnetosphere, and the dynamics of particle acceleration at work in these astrophysical particle accelerators. To achieve this goal, I propose to study their gamma-ray radiation through a search for new VHE-emitting pulsars with the most sensitive VHE instrument in the northern hemisphere for point-like

targets. In this project I will analyze gamma-ray data from different types of pulsars including: millisecond pulsars (MSPs); pulsars in binary systems; and young, bright pulsars. I will also conduct a search for VHE emission from 13 pulsars that appear in archival VERITAS data, which will represent the first time that any of the 13 pulsars have been analyzed in the VHE band.

1.2. Experimental technique and analysis methods

The imaging atmospheric Cherenkov telescope technique involves the detection of the bluish Cherenkov photons produced in cosmic ray and gamma-ray initiated air showers. When a gamma ray of cosmic origin enters the upper Earth atmosphere, it interacts with a nucleus of an atmospheric molecule to produce an electron-positron pair (pair production). The charged particles produced in the shower exceed the speed of light in air and thus radiate Cherenkov photons. Further, these charged particles re-interact with other nuclei in the air via the bremsstrahlung mechanism and radiate more gamma rays, which themselves can then pair produce. A cascade or "air shower" quickly forms with many charged particles careening toward the Earth's surface while radiating Cherenkov photons. The angle for emission of Cherenkov photons in air is roughly 1.4°, and the resulting few-nanosecond-long flash of Cherenkov light on the ground has a typical light pool radius of about 100 m for a 1 TeV gamma-ray shower.

The VERITAS array of four 12 m diameter IACTs is located in Arizona at the base of Mt. Hopkins and has been operation since 2007. The telescope reflectors each consist of 345 hexagonal mirror facets, and the cameras comprise 499 photomultiplier tubes (PMTs) with a field of view of $\sim 3.5°$. VERITAS is sensitive to gamma-ray photons in the energy range ~ 0.1–30 TeV with an energy resolution of $\sim 15\%$ and an angular resolution of $0.15°$ (Holder et al. 2008). A major upgrade effort was completed in summer 2012 of which I was a part for four weeks. Each of the $\sim$ 2000 PMTs were replaced by new, higher efficiency Hamamatsu photomultiplier tubes, which has had the effect of reducing the lower energy threshold of the array to below 0.1 TeV and increasing the photon detection efficiency by a factor of $\sim 50\%$ (D. B. Kieda for the VERITAS Collaboration 2013).

Current-generation IACTs use fast and very sensitive PMTs to detect these Cherenkov photons by turning the light into an electric signal that can subsequently be digitized and characterized in an offline analysis. The VERITAS telescopes consist of a large, segmented concave reflector that focuses the light onto the PMT camera. An electronic trigger system is used to ensure the recording of air shower light by selectively reading out the array when a group of neighboring PMTs have each seen enough light to produce a signal above the trigger threshold. In the case of multiple telescopes, the PMT signals will only be read out when two or more neighboring telescopes have been triggered within a 50-nanosecond time window.

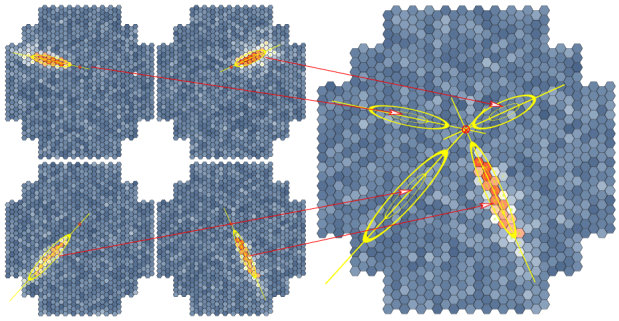

Fig. 2.— Example of how the imaged Cherenkov light produced in a one gamma-ray induced air shower appears in the telescope cameras. The rightmost image shows how superposing the elliptical gamma-ray signitures allows for computation of the origin of the gamma ray in the camera plane. Figure from (Völk & Bernlöhr 2009).

The imaging atmospheric Cherenkov technique opened a new window to the universe with the detection of the Crab Nebula in 1989, but it would not have been possible without the many efforts in the development of the imaging technique. The vast majority of the recorded data is due to cosmic-ray triggers. In fact, these cosmic-ray triggers outnumber gamma-rays by 1000:1, underscoring the need for understanding the properties of each type of image that appears in the data to properly remove the cosmic-ray background. Gamma-ray images appear in the camera as ellipses due to the more narrow nature of an electromagnetically induced shower (see Figure 2). Cosmic-ray initiated showers allow the production of more hadrons that are not as confined in the transverse direction, and so the shower progression has more spread creating images in the cameras that are more irregularly shaped, not narrow and elliptical. Application of a principle moment parameterization is done in the offline data analysis, which characterizes the properties of the elliptical images to suppress $\sim 99\%$ of the background due to cosmic rays and allows reconstruction of the gamma-ray energy and arrival direction (Hillas 1985).

2. COMPLETED AND ONGOING WORK

2.1. Searches for pulsed emission from pulsars in the VHE band

2.1.1. Geminga

Formally known as PSR J0633+1746, the Geminga pulsar (henceforth referred to as Geminga) is located at the relatively close distance of 250 pc and is the second brightest steady high-energy (HE; $E > \sim 100$ MeV) gamma-ray source in the sky. It is the first GeV-emitting pulsar detected with no known radio counterpart (Bertsch et al. 1992). Geminga has a spin period of ~ 240 ms and a spin-down luminosity of 3.2×10^{34} erg s^{-1}.

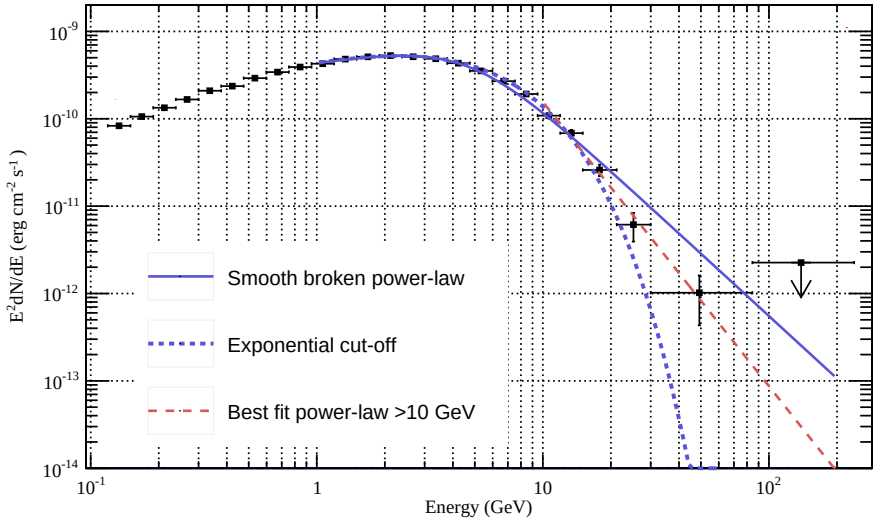

Fig. 3.— Phase-resolved *Fermi*-LAT SED for the Geminga pulsar. Three fits have been applied to the data: a smooth broken power law (solid blue line), a power law with an exponential cutoff (dotted blue line), and a simple power law above 10 GeV. Fitting the tail of the spectrum with an exponential cutoff and power law above 10 GeV revealed fit probabilities of 80% and 85%, respectively.

Similar to the Crab in the high-energy band, Geminga shows a double-peaked phaseogram separated by a "bridge" of emission above the background, with only one of the peaks remaining dominant above about 10 GeV. As has been seen in the past for other *Fermi*-LAT detected pulsars, the spectrum of Geminga above 100 MeV is well-described by a power law with an exponential cut-off (Abdo et al. 2013), characteristic of the curvature radiation processes thought to dominate in the magnetosphere as described in Section 1.1.

Motivated by the Crab pulsar detection in the VHE band and its extended power-law spectral tail into the VHE regime (see Section 1.1), I have performed a spectral analysis of ~ 4.5 yrs of *Fermi*-LAT data and analyzed all of the VERITAS data on Geminga that has been taken. The *Fermi*-LAT data were analyzed with `Science Tools v9r27p1` with `P7V6` instrument response functions and the standard quality cuts described in Nolan et al. (2012). A cut on event phases is applied to select only those events coincident with the main peak of pulsed emission. The pulsar timing solution used was obtained from the public *Fermi*-LAT pulsar ephemerides webpage[2]. A spectral analysis with 27 logarithmically spaced energy bins between 100 MeV and 300 GeV was subsequently performed. The resulting spectrum with fits can be seen in Figure 3. In the tail of the spectrum above

[2]http://fermi.gsfc.nasa.gov/ssc/data/access/lat/ephems/

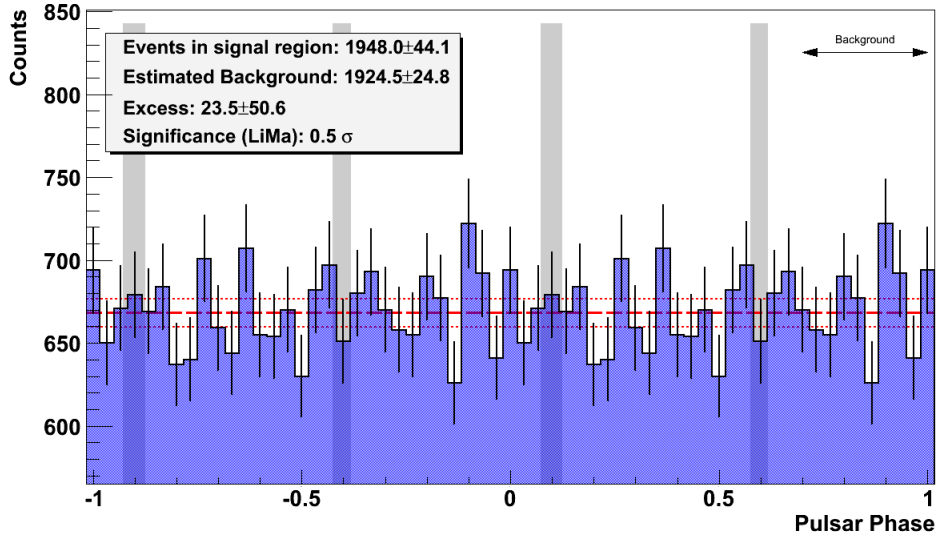

Fig. 4.— VERITAS light curve for the Geminga pulsar with events phase-folded using a publicly available *Fermi*-LAT ephemeris and an XMM-*Newton* timing solution provided in a private communication. The grey bands represent the expected signal regions as defined by the full width at half max. (FWHM) of Gaussian fits to the peaks in the *Fermi*-LAT phaseogram (not shown). The phase regions are [0.072 - 0.125] and [0.575 - 0.617] for P1 and P2, respectively. The background region is defined as [0.7 - 1.0] where no pulsed or bridge emission is seen in the *Fermi*-LAT light curve. The reported significance using these defintions of the signal and background regions is 0.5σ, implying no detection of pulsed VHE emission from Geminga.

10 GeV, the simple power-law fit to the data is comparable to the exponential cutoff, with fit probabilities of 85% and 80%, respectively.

The VERITAS data were analyzed in the pipeline as described in Section 1.2. The data span three different configurations of the VERITAS array over ~ 6 yrs: before and after the relocation of one telescope, and after the summer 2012 upgrade of the cameras with higher effeciency PMTs. While the *Fermi*-LAT ephemeris was found to be valid for phase-folding all VERITAS observations taken after the launch of *Fermi*, the 2007 season data collected before the relocation of Telescope 1 were phase-folded using an XMM-*Newton* timing solution provided by Dr. Eric Gotthelf via private communication. The two gamma-ray peaks in the *Fermi*-LAT pulsar light curve, P1 and P2, were selected as signal regions for the VERITAS search, while the phase region [0.7 - 1.0] was defined as background. The resulting VHE phaseogram for the Geminga pulsar is shown in Figure 4 and reveals no hint of pulsed emission in the VHE band. The *H*-test (de Jager et al. 1989), which tests for periodicity in sparsely sampled light curves, was also employed to search for periodic emission in the VHE phaseogram, revealing an H statistic of 0.58 that corresponds to an insignificant random-chance probability of 79%. Finally, 99% confidence-level integral flux

upper limits were computed with the method of Helene (1983) above 135 GeV for both P1 and P2 to constrain a possible hard component in the pulsar SED. The two flux ULs for P1 and P2 are $6.44 \times 10^{-13}\,\mathrm{cm}^{-2}\,\mathrm{s}^{-1}$ and $4.34 \times 10^{-13}\,\mathrm{cm}^{-2}\,\mathrm{s}^{-1}$, respectively.

A paper is currently in preparation for the search for pulsed VHE emission from the Geminga pulsar with Dr. Andrew McCann and myself as lead authors. The paper is expected to be published as a letter before the end of 2014.

2.1.2. PSR B1937+21

PSR B1937+21 (henceforth PSR B1937 or B1937) is the first millisecond pulsar (MSP; $P \lesssim 30\,\mathrm{ms}$) ever discovered and has the shortest spin period ($P \simeq 1.56\,\mathrm{ms}$) of any known pulsar observable with VERITAS (Backer et al. 1982). Its distance is not firmly known due to uncertainty in the dispersion model and has been reported as both $\sim 3.6\,\mathrm{kpc}$ (Brisken et al. 2002) and $\sim 7.7\,\mathrm{kpc}$ (Verbiest et al. 2009). It is in several ways similar to the Crab pulsar, which make PSR B1937 a possibly auspicious candidate for pulsed VHE emission. Firstly, it is one of very few known pulsars to exhibit giant radio pulses; in fact, the giant pulses from B1937 are the brightest radio emission ever detected from anywhere in the universe (Soglasnov et al. 2004). Secondly, the pulsed X-ray spectrum of B1937 is non-thermal and quite hard with $\Gamma = 1.14 \pm 0.07$ (Cusumano et al. 2003), and these X-ray photons could be inverse-Compton scattered into the TeV regime. Finally, the peaks in the radio phaseogram are slightly offset from the X-ray peaks just as in the Crab pulsar light curves. PSR B1937 is a *Fermi*-LAT pulsar that has been detected with a significance of 7.2σ, and its phase-averaged gamma-ray SED reveals a photon index between 0.5 and 5 GeV of $\Gamma = 1.43 \pm 0.87$ with a cutoff energy at $\sim 1.2\,\mathrm{GeV}$ (Guillemot et al. 2012). As explained in Section 1.1, a VHE component in the SED could either be an extension of the pulsar spectral tail or a new inverse-Compton component due to upscattering of photons in the magnetosphere by relativistic electrons.

A search for pulsed VHE emission from the direction of PSR B1937+21 is currently underway with VERITAS, and I am the lead investigator. A proposal I authored for VERITAS time on B1937 was successful in procuring 30 hrs during the past 2013/2014 VERITAS observing cycle. The observations were recently completed on 2 July 2014, and I have analyzed all of the data obtained. The phase-folding was accomplished by using a publicly available *Fermi*-LAT timing solution whose validity was verified for the 2014 VERITAS data by confirming linear growth of the H statistic in folding contemporaneous *Fermi*-LAT data for B1937. The expected signal regions in the VHE phaseogram were defined corresponding to the peaks in the X-ray light curve, as a signal above $\sim 1\,\mathrm{TeV}$ would possibly be upscattering of the X-ray photons. Using this definition for the signal regions, the anlysis reveals marginal evidence for pulsed emission at the 2.6σ level; see Figure 5. A 25-hr follow-up campaign is expected to take place during the 2014/15 cycle,

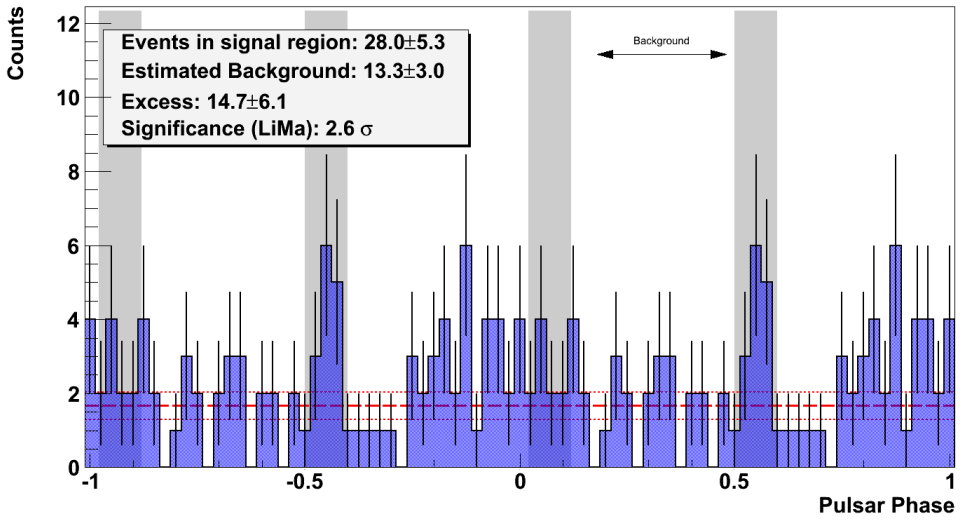

Fig. 5.— Millisecond pulsar PSR B1937+21 light curve of VHE events phase-folded with the public *Fermi*-LAT ephemeris. The light curve contains 40 bins and shows two pulsar periods. The "on" regions (grey bands) were chosen to correspond to P1, P2 in the X-ray phaseogram. All 30 hrs of observations were used in generating this phaseogram.

and I will be lead author for a VERITAS collaboration paper that will be published in 2016.

2.1.3. PSR J1023+0038

The system FIRST J102347.6+00384 in an eclipsing binary system that was recently discovered to contain an MSP with a very fast period of 1.69 ms orbiting a non-degenerate companion star in a ~ 4 hr orbit, found in a survey by the Green Bank Telescope (Archibald et al. 2009). Before the discovery of the MSP, in 2001 the system was identified as a low-mass X-ray binary (LMXB) with an accretion disk (Thorstensen & Armstrong 2005). Later, optical and X-ray observations revealed the disappearance of the accretion disk, implying a state change to the MSP state (Woudt et al. 2004). However, much to the surprise of the astronomical community, in 2013 June the radio pulsations disappeared (Stappers et al. 2013) and the system was shown to have reformed an accretion disk (Halpern et al. 2013), thus reverting back to the LMXB phase and constituting the first time a system has been seen to oscillate between the two states.

This binary system is a promising candidate for VHE emission for two reasons: a) the presence of an MSP and b) NS-B star binary systems with shocked material have been seen as VHE emitters in the past (e.g. LS I +61°303, Acciari et al. (2008)). In this project I have focused on the search for pulsed VHE emission from the MSP, while collaborator Dr. Ester Aliu has performed the search for steady and modulated VHE gamma-rays from the

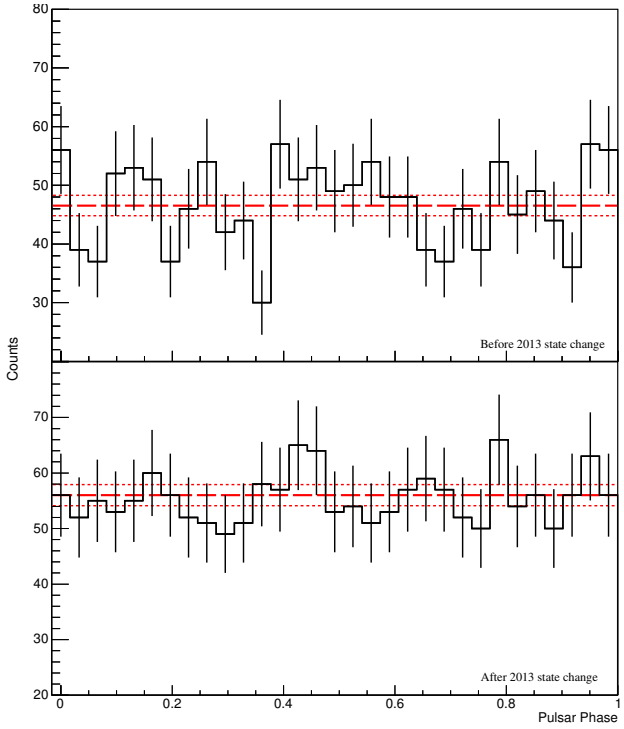

Fig. 6.— Phaseograms of VHE events that were phase-folded with the Jodrell Bank radio ephemeris. The top panel shows the light curve for all VERITAS data taken before the disappearance of the radio pulsar, while the bottom panel shows the light curve for data taken after the disappearance. The solid and dashed red lines are the average number of counts and error on the average, respectively.

system. The search for pulsed VHE emission was split into two parts as VERITAS data was taken both before and after the 2013 June disappearance of the radio pulsar (henceforth these epochs are referred to as 'pre-' and 'post-state change'). The VERITAS observation time accumulated on the target is 18.1 hrs pre- and 8.2 hrs post-state change. Events were phase-folded using a Jodrell Bank radio ephemeris that was provided in a private communication by A. Archibald, though the location of phase zero is unknown, precluding the possibility of defining on regions in the phaseogram. Hence, for this analysis de Jager's *H*-Test is employed to compute *H* statistics that reflect the probability of the presence of a periodic signal in the data. The *H*-Test does not reveal any hint of periodicity in the VHE phaseograms, which are shown in Figure 6. The *H* statistics are used to compute 2 and 3σ upper limits via the method of de Jager (1994) above an energy threshold of 166 GeV assuming a duty cycle of 10% and Gaussian pulse shapes. The computed 2σ flux ULs are $6.2 \times 10^{-9}\,\mathrm{m}^{-2}\ \mathrm{s}^{-1}$ and $1.12 \times 10^{-8}\,\mathrm{m}^{-2}\ \mathrm{s}^{-1}$ for the pre- and post-state change data, respectively. Dr. Aliu and I act as lead authors on a VERITAS collaboration publication that is currently in preparation and will be published before the end of 2015.

2.2. Search for correlated HE-VHE gamma-ray variability during a bright Crab Nebula flare

Despite being perhaps the best-studied particle accelerator, the Crab Nebula has posed interesting challenges to scientists. One of the current mysteries of the Crab Nebula is the recent detection of gamma-ray flares by the AGILE and *Fermi*-LAT collaborations (Tavani et al. 2011), (Abdo et al. 2011). The detection of these flares contradicted the erstwhile steady-emmission paradigm that had been established by the then-accepted magnetohydrodynamic framework with the pulsar as the central engine (Rees & Gunn 1974). Further, no correlated flaring has been reported in any other energy band (Horns et al. 2010), (Weisskopf 2013), though coverage at VHEs has been rather sparse. In this project I have completed an analysis of VHE observations of the Crab Nebula during a flaring episode that took place in 2013 March.

VERITAS observations of the Crab Nebula were triggered in early March by an automated *Fermi*-LAT analysis pipeline that has been established by collaborator Dr. Manel Errando at Columbia University-Barnard College. The automated pipeline employs a model of the HE gamma-ray emmission from the Crab Nebula and pulsar that I generated. VERITAS observations of the nebula continued for ten days during the flare, which spanned a two week period. The HE gamma-ray flux was elevated by an average factor of ~ 6, but the VHE data do not reveal any correlated flux enhancement above 1 TeV (see Figure 7). A 95% confidence level UL is computed by a Bayesian approach in which the prior assumption that the VHE flux was elevated above its average value by at least some non-negative factor is invoked. The calculated UL constrains an elevated average VHE flux to be at most 5.3% with 95% confidence. Finally, a constraint on a correlated HE-VHE linear flux enhancement is computed, and the resulting linear correlation factor is found to be at most 8.6×10^{-3} with the same confidence. I was lead author for the VERITAS collaboration paper reporting these findings that was published in The Astrophysical Journal Letters in early 2014 (Aliu et al. 2014).

2.3. Probing the VERITAS signal chain with a picosecond pulsed laser

The goal of this project was to determine and quantify idiosyncrasies (e.g. nonlinear effects) in the electronics chain used on site at VERITAS. This chain comprises the photomultiplier tube (PMT) and the flash analog-to-digital converter (FADC) used to digitize the analog signal pulses from the PMT. When Cherenkov light from an air shower enters a PMT on site at VERITAS, the resulting analog pulse is digitizied in an FADC system that was designed and fabricated by Prof. Jim Buckley's group at Washington University at St. Louis. In an effort to extend the dynamic range of the digitizer, the Wash U. group developed electronics to attenuate pulses with amplitudes above some reference voltage at the FADC, called the low-gain switch. As the switch comprises analog electronic

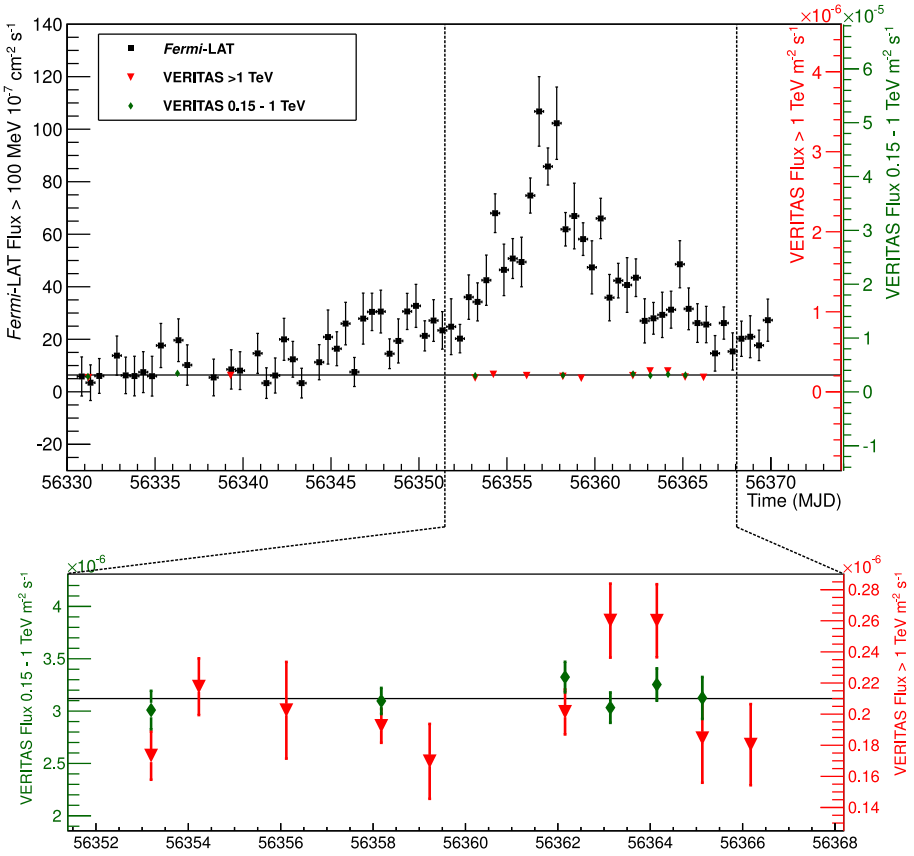

Fig. 7.— *Fermi*-LAT and VERITAS light curves for the 2013 March Crab Nebula flare. The VERITAS light curves (triangle and diamond markers) span ten nights during the flare. The baseline Crab Nebula synchrotron flux above 100 MeV and average VHE flux above 0.15 TeV and 1 TeV are aligned and are indicated by the solid black line. No correlated variability with the flux > 100 MeV is evident in the VERITAS light curve.

elements, it not surprisingly has sub-optimal characteristics that must be understood and quantified for the development of accurate simulations for use in data analysis. In order to achieve this goal, I have conducted a measurement at Wash U. involving tracking the shapes and amplitudes of test pulses throughout the VERITAS electronics chain.

In this project, a PicoQuant 638 nm pulsed laser (model LDH 8-1-469) was triggered at 200 Hz by a Stanford delay/pulse generator (model DG535). The laser fired picosecond pulses of red light through a series of up to three Edmund Optics non-reflective visible neutral density filters (model 64-352) into a VERITAS PMT. All of the aforementioned components were secured to a black breadboard using optical mounts. The PMT preamplifier was biased at ± 5 V; the high-voltage was set to 800 V for the PMT. The charge-injection line was terminated at 50 Ω to avoid signal pickup. The coax signal

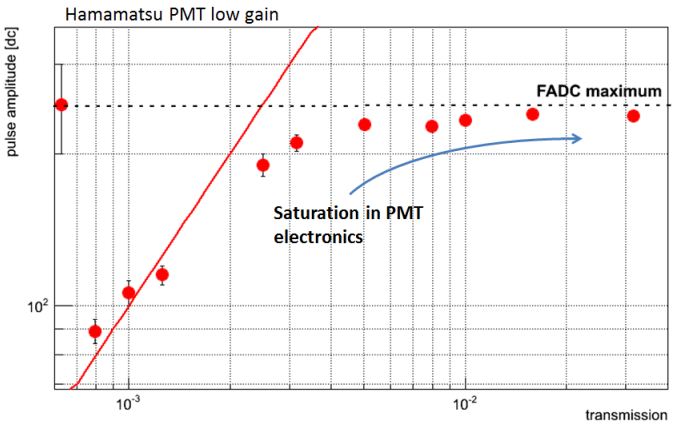

Fig. 8.— Low-gain amplitude response across increasing levels of light for the Hamamatsu PMT. The red points are computed by adopting one recorded trace as a template, fitting each trace for the given optical density with a Gaussian, and time-shifting and amplitude-scaling to best match the template trace before averaging. The pulse amplitudes clearly do not follow the linear progression that has been assumed in VERITAS simulations in the past.

cable was connected to a spare 75 Ω VERITAS cable, which connected to the FADC or oscilloscope with 75 Ω terminator. A flat-black metal casing was placed over the components on optical mounts to ensure darkness in the enclosure. Lastly, a black cloth was placed over the enclosure to further reduce contamination by stray light. Traces from the PMT for each optical density configuration were recorded on the oscilloscope before being recorded in the FADC. Ten traces in the FADC were recorded for each configuration, and 128 samples were read out for each recorded pulse. The average pulse amplitude for each configuration was then calculated by assuming one pulse as a template and then aligning the other pulses for averaging, which eliminates effects due to timing jitter. The analysis was done by Prof. Nepomuk Otte while I performed the data collection at Wash U.

The two main findings of this study are: a) saturation of pulses at 255 digital counts in the high-gain regime of the FADC and b) nonlinearity in the low-gain regime (see Figure 8). The nonlinearity of the low-gain is an issue that must be addressed for proper energy reconstruction above ~ 1 TeV, since in the past simulations have assumed a linear response. A new system that uses the pulse shape templates that I recorded to account for the nonlinearity is currently being implemented in the Camera and Optics Readout (CARE) simulation package with promising preliminary findings.

3. FUTURE WORK

3.1. Search for pulsed VHE emission in archival VERITAS pulsar data

The detection of even one new pulsar in the VHE gamma-ray band would be a crucial finding for our augmenting our understanding of the physics of pulsar emission. In the ongoing effort to extend the list of VHE-detected pulsars to beyond just the Crab, I will complete the analysis of 13 *Fermi*-LAT detected pulsars that all appear in archival VERITAS data; see Table 1 for a list of these pulsars (plus Geminga) and some of their relevant characteristics. There are currently no reports in the literature that any of the pulsars listed other than Geminga have been observed in the VHE band in the past; therefore, this analysis will in the case of new detections or in the case of none provide novel and valuable information about particle acceleration in the pulsar magnetosphere.

Quoted in the Flux column of Table 1 for each pulsar is the flux between 10 and 100 GeV from the 2FGL, and the final column shows the expected VHE flux relative to the Crab pulsar flux above 100 GeV from a power-law extrapolation of the 2FGL spectrum. While the detection of one or more of the pulsars is certainly possible at the level of what is quoted in the Limit column, it is an over-auspicious outlook for two reasons: a) the exact spectral shape is unknown – is it really just a power law? and b) the power-law extrapolation itself is subject to uncertainty due to sparse statistics in the *Fermi*-LAT data above 10 GeV. However, in addition to performing an analysis targeting potential emission at the level of the extrapolations, I will also complete an analysis for each pulsar that is sensitive to emission around an energy of 1 TeV, which is where several recent theoretical models have predicted the appearance of an inverse-Compton component in the pulsar SEDs (e.g. Lyutikov et al. (2012), Aharonian et al. (2012)).

All aspects of the aforementioned analyses should take roughly one year total to complete, with each pulsar requiring about a one-month turn-around time. I will complete the analysis along with colleague Dr. Andrew McCann. I have shown through my previous pulsar analyses that I can analyze pulsar data on relatively short timescales, aided by the fact that all of the necessary tools are currently in place. In the case that one or more of these pulsars display a hint of emission at a level above $\sim 2.5\sigma$, I have demonstrated that I am capable of successfully requesting follow-up observations with VERITAS and publishing an analysis in the peer-reviewed literature. Publication plans for this project remain tentative as we do not know exactly what we will find once we unblind ourselves to the data.

Name	$\dot{E}$ [ergs/s]	T_{obs} [hrs]	T_{eff55} [hrs]	Pulse FWHM [% of Crab]	$Flux_{10\_100GeV}$ [cm^{-2} s^{-1}]	Limit [% of Crab]
PSR J0633+0632	1.2×10^{35}	119.0	90.1	46.4	1.89×10^{-11}	13.1
PSR J0248+6021	2.1×10^{35}	106.6	49.2	87.7	9.53×10^{-11}	24.4
PSR J2021+3651	3.4×10^{36}	91.4	72.4	32.4	3.43×10^{-10}	12.2
PSR J2032+4127	2.7×10^{35}	82.9	48.3	33.7	3.63×10^{-10}	15.3
PSR J1907+0602	2.8×10^{36}	79.7	54.9	87.7	3.37×10^{-10}	23.1
PSR J2030+3641	3.2×10^{34}	75.6	19.0	127.1	6.65×10^{-11}	47.4
PSR J2021+4026	1.2×10^{35}	74.0	36.7	109.6	5.58×10^{-10}	31.7
PSR J2229+6114	2.2×10^{37}	68.2	47.05	100.8	2.13×10^{-09}	26.8
PSR J0633+1746	3.2×10^{34}	55.8	54.95	42.5	2.8×10^{-09}	16.1
PSR J0007+7303	4.5×10^{35}	35.6	0	153.5	1.24×10^{-09}	-
PSR J0205+6449	3.0×10^{37}	19.3	9.7	122.8	1.37×10^{-10}	65.2
PSR J0659+1414	3.8×10^{34}	15.3	9.7	87.7	7.67×10^{-11}	55.0
PSR J2030+4415	-	14.3	14.2	57.0	1.04×10^{-10}	67.2
PSR J0631+1036	1.7×10^{35}	13.0	13.0	109.6	1.11×10^{-10}	53.2

Table 1: A list of 14 young pulsars for which there exists archival VERITAS data. The T_{obs} column lists the total four-telescope VERITAS time in hours that has been collected, while T_{eff55} gives the total time that the target was above 55° in elevation and further applying a correction for acceptance. The Pulse FWHM column gives the sum of the widths of the pulse peaks in the phaseogram as a percentage of that for the Crab pulsar. $Flux_{10\_100GeV}$ is the flux between 10 and 100 GeV that is reported for the source in the 2FGL catalog Nolan et al. (2012). The last column lists a 95% CL limit estimate for the integral flux above 100 GeV as a percentage of Crab pulsar flux by extrapolation of a power-law fit to the *Fermi*-LAT data. This table was compiled by collaborator Dr. Andrew McCann (U. Chicago).

3.2. Analysis of a possibly new extended VHE source in the PSR B1937+21 field of view

The pointing used for data collection on PSR B1937+21 was offset from the pulsar to allow for simultaneous observations of HESS J1943+213, an interesting blazar-like, HESS-identified source. In the analysis of the HESS source led by Dr. Karsten Berger, a $\sim 6\sigma$ extended hot spot about 1° from the center of the FoV was identified. There are two pulsars that have been identified very near to the hot spot: PSR J1936+21 and PSR J1935+2025, making it possible that the hot spot is a hitherto unidentified VHE-emitting PWN. As I have already processed all of the data taken so far on this pointing, I volunteered to perform a secondary analysis with a separate analysis package. Preliminary findings show a $\sim 4\sigma$ excess at the same location, though I will perform a proper extended-source analysis in addition to a search for VHE pulsations from the location of both pulsars. Follow-up observations will be requested for the upcoming 2014/2015 observing cycle, and in the case of a firm detection of a new VHE source, a publication is expected by the end of 2015.

3.3. Verifying the VERITAS Monte Carlo simulation chain by data comparison

As a natural extension of the VERITAS signal chain testing I completed in 2013 December, I plan to complete a project in which I will validate the Monte Carlo simulations used in data analysis by comparison with actual VERITAS data. Having robust and accurate Monte Carlo simulations of the electronic response of VERITAS to the Cherenkov light produced in air showers is essential for properly reconstructing all of the physical parameters of the primary gamma-ray that initiated the shower. A poorly simulated IACT will be plagued by systematic errors.

The Camera and Readout Electronics (CARE) Monte Carlo simulation package is one of a few similar packages used in VERITAS analysis, and it has recently implemented the pulse shape templates that I recorded on all original hardware at Wash U. (see Section 2.3 for more detail) with promising preliminary results. However, there is still work to be done in validating all of the relevant aspects of the simultations for use in analysis. This project will focus on achieving four interrelated goals:

1. Fine tuning simulations to match the response of the electronics
2. Comparison of high-level Monte Carlo simulation parameters with those seen in reconstructed data
3. Production of simulations for all VERITAS observing modes
4. Quantifying the systematic uncertainty on energy.

The problem of matching the nonlinear response of the electronics in the low-gain is mainly in deciding when and how to switch templates (the red points in Figure 8). As of this writing CARE has implemented a linear interpolation between template pulse shapes, but this method ignores the fact that the region in between the measured pulse shapes is nonlinear. A more sophisticated interpolation may prove necessary to achieve an acceptably low systematic uncertainty on the reconstructed energy, which is important in the case that a new pulsar component $> 1\,\mathrm{TeV}$ is detected in the proposed project.

Comparison of high-level Monte Carlo simulation parameters with those seen in reconstructed data involves comparison of the computed parameters from the moment analysis (e.g. mean scaled width, mean scaled length, size, etc.) with those found from simulated gamma-ray showers. Furthermore, the simulation package must accurately produce sims for all of the various observing modes of VERITAS, which implies simulation of the instrument response for various wobble offsets, on/off observing modes, and different atmospheric conditions. It is clear that this project is of paramount importance for proper gamma-ray reconstruction in the offline analysis.

REFERENCES

Abdo, A. A., Ackermann, M., Ajello, M., et al. 2011, Science, 331, 739

Abdo, A. A., Ajello, M., Allafort, A., et al. 2013, ApJS, 208, 17

Acciari, V. A., Beilicke, M., Blaylock, G., et al. 2008, ApJ, 679, 1427

Aharonian, F. A., Bogovalov, S. V., & Khangulyan, D. 2012, Nature, 482, 507

Aliu, E., Archambault, S., Aune, T., et al. 2014, ApJ, 781, L11

Archibald, A. M., Stairs, I. H., Ransom, S. M., et al. 2009, Science, 324, 1411

Backer, D. C., Kulkarni, S. R., Heiles, C., Davis, M. M., & Goss, W. M. 1982, Nature, 300, 615

Bertsch, D. L., Brazier, K. T. S., Fichtel, C. E., et al. 1992, Nature, 357, 306

Brisken, W. F., Benson, J. M., Goss, W. M., & Thorsett, S. E. 2002, ApJ, 571, 906

Cheng, K. S., Ho, C., & Ruderman, M. 1986, ApJ, 300, 522

Cusumano, G., Hermsen, W., Kramer, M., et al. 2003, A&A, 410, L9

D. B. Kieda for the VERITAS Collaboration. 2013, ArXiv e-prints, arXiv:1308.4849

de Jager, O. C. 1994, ApJ, 436, 239

de Jager, O. C., Raubenheimer, B. C., & Swanepoel, J. W. H. 1989, A&A, 221, 180

Guillemot, L., Johnson, T. J., Venter, C., et al. 2012, ApJ, 744, 33

Halpern, J. P., Gaidos, E., Sheffield, A., Price-Whelan, A. M., & Bogdanov, S. 2013, The Astronomer's Telegram, 5514, 1

Helene, O. 1983, Nuclear Instruments and Methods in Physics Research, 212, 319

Hillas, A. M. 1985, International Cosmic Ray Conference, 3, 445

Holder, J., Acciari, V. A., Aliu, E., et al. 2008, in American Institute of Physics Conference Series, Vol. 1085, American Institute of Physics Conference Series, ed. F. A. Aharonian, W. Hofmann, & F. Rieger, 657–660

Horns, D., Tennant, A., Ferrigno, C., et al. 2010, The Astronomer's Telegram, 3058, 1

Lyutikov, M., Otte, N., & McCann, A. 2012, ApJ, 754, 33

Nolan, P. L., Abdo, A. A., Ackermann, M., et al. 2012, ApJS, 199, 31

Rees, M. J., & Gunn, J. E. 1974, MNRAS, 167, 1

Soglasnov, V. A., Popov, M. V., Bartel, N., et al. 2004, ApJ, 616, 439

Stappers, B. W., Archibald, A., Bassa, C., et al. 2013, The Astronomer's Telegram, 5513, 1

Tavani, M., Bulgarelli, A., Vittorini, V., et al. 2011, Science, 331, 736

Thorstensen, J. R., & Armstrong, E. 2005, AJ, 130, 759

Verbiest, J. P. W., Bailes, M., Coles, W. A., et al. 2009, MNRAS, 400, 951

VERITAS Collaboration, Aliu, E., Arlen, T., et al. 2011, Science, 334, 69

Völk, H. J., & Bernlöhr, K. 2009, Experimental Astronomy, 25, 173

Weekes, T. C., Cawley, M. F., Fegan, D. J., et al. 1989, ApJ, 342, 379

Weisskopf, M. C. 2013, Mem. Soc. Astron. Italiana, 84, 582

Woudt, P. A., Warner, B., & Pretorius, M. L. 2004, MNRAS, 351, 1015